Patient-Specific, 3-Dimensional Dosimetry in Non-Hodgkin's Lymphoma Patients Treated with ^{131}I-anti-B1 Antibody: Assessment of Tumor Dose–Response

George Sgouros, PhD; Shannon Squeri, BA; Åse M. Ballangrud, PhD; Katherine S. Kolbert, MS; Jerrold B. Teitcher, MD; Katherine S. Panageas, PhD; Ronald D. Finn, PhD; Chaitanya R. Divgi, MD; Steven M. Larson, MD; and Andrew D. Zelenetz, MD, PhD

Memorial Sloan-Kettering Cancer Center, New York, New York

A comprehensive, SPECT-based, patient-specific 3-dimensional (3D) dosimetry analysis has been performed using 3D-ID, a previously developed software package. The role of the total-body tumor burden, individual lesion size, tumor absorbed dose, and the spatial distribution of the absorbed dose on response and on the time course of tumor shrinkage has been examined in patients with lymphoma treated by radioimmunotherapy. **Methods:** Data from 15 patients participating in a phase II study of ^{131}I-labeled anti-B1 antibody (tositumomab) were used. Patients were administered a tracer dose of ^{131}I for imaging and pharmacokinetics. Dose estimates from the tracer studies were used to prescribe the therapeutic administration such that the whole-body absorbed dose did not exceed 75 cGy. All patients received a fixed mass amount of antibody for both the tracer and the therapeutic administrations. SPECT and planar imaging were performed 3–4 d after the therapeutic administration. CT or MRI scans were available on all patients. Total tumor burden was assessed by drawing contours around all lymphoma lesions identified on whole-body CT or MRI. Mean absorbed doses were estimated for selected, index lesions by conventional dosimetry and also by 3D SPECT-based dosimetry. Using a patient-specific dosimetry package, 3D-ID, dose–volume histograms were also generated to assess the spatial distribution of absorbed dose. This approach made it possible to obtain estimates of the minimum and maximum absorbed doses for individual tumors in addition to the mean. **Results:** Mean absorbed dose estimates obtained by patient-specific SPECT-based dosimetry using 3D-ID were within 2%–5% of estimates obtained by conventional dosimetry. None of the absorbed dose parameters (mean, minimum, maximum, uniformity) were found to have a significant correlation with tumor response. The total-body tumor burden did not impact on overall response or toxicity. **Conclusion:** This analysis represents the first full reported implementation of a patient-specific 3D dosimetry package. The absence of a dose–response relationship for tumors is surprising and suggests that absorbed dose is not the sole determinant of tumor response in these patients. The absence of a correlation between the total-body tumor burden and overall response or toxicity suggests that tailoring the milligram amount of administered antibody to patient tumor burden is not likely to improve response or reduce toxicity.

Key Words: radioimmunotherapy; patient-specific dosimetry; 3D-ID software; tumor dose–response

J Nucl Med 2003; 44:260–268

Radiolabeled antibody therapy has been most successful in the treatment of non-Hodgkin's lymphoma (NHL) (*1*,*2*). At an advanced stage, when conventional therapy is ineffective (*3*), radioimmunotherapy, using (anti-CD20) antibodies, labeled with ^{131}I or with ^{90}Y, has been consistently and reproducibly effective against this disease (*1*,*2*,*4*–*7*). Recent studies have shown that as a first-line therapy the effectiveness increases considerably (*8*).

The objective of this work was to determine which of several parameters most impacted on tumor response in NHL patients treated with ^{131}I-anti-B1 radioimmunotherapy and also to examine whether therapeutic efficacy would improve if the treatment protocol were made patient specific in terms of the milligram amount of antibody administered. ^{131}I-anti-B1 radioimmunotherapy of lymphoma is currently conducted using 2 very different approaches. Both approaches rely on treatment planning to specify the administered amounts for treatment. The approach used at the University of Washington, Seattle, allows for the administration of close to gigabecquerel (curie) levels of ^{131}I-anti-B1 antibody with planned stem cell support (*2*). The therapeutic dose is preceded by administration of unlabeled anti-B1 antibody. The radioactivity given each patient is based on a series of pretherapy tracer studies that are used to obtain pharmacokinetics for dosimetry (*9*). In a similar patient population, a nonmyeloablative approach that does not require stem cell support has been developed by Ka-

Received Jan. 10, 2002; revision accepted Sep. 17, 2002.

For correspondence or reprints contact: George Sgouros, PhD, Department of Medical Physics, Memorial Sloan-Kettering Cancer Center, 1275 York Ave., New York, NY 10021.

E-mail: sgourosg@mskcc.org

minski et al. (*1,5,10*) at the University of Michigan. In the Michigan approach, treatment is implemented by first administering a fixed amount of unlabeled antibody followed by trace-labeled antibody, and the whole-body residence times are determined (*11,12*). From these tracer dose measurements, the amount of radioactivity necessary to deliver 65 or 75 cGy, whole body (the maximum tolerated dose for hematologic toxicity obtained from a phase I trial), is determined. The whole-body absorbed dose calculations are performed using pharmacokinetic data collected the week before therapy (*11*).

Pretherapy administration of unlabeled antibody has been an important element in the success of radiolabeled anti-B1 antibody treatment of NHL in both the Michigan and Seattle approaches. In both approaches, the administered radioactivity is based on each patient's pharmacokinetics. In contrast to the adjustments made for radioactivity, the protein mass of antibody has been kept constant across patients. Preceding the radiolabeled antibody administration with unlabeled antibody is thought to saturate nonspecific uptake in the reticuloendothelial system or antigen sites on readily accessible, circulating B-cells, but not on less rapidly accessible tumor-associated sites. Such a strategy will be most successful when a balance is obtained between administering the amount of antibody required to saturate sites that are not tumor associated while ensuring that tumor-associated sites are also not saturated. Because the number of tumor sites will depend on tumor bulk, it may be expected that individual patient tumor volume will impact on this balance, requiring that the amount of unlabeled antibody be adjusted according to estimated tumor burden for each patient. Both preclinical and clinical evidence exist to suggest that tumor bulk has an impact on pharmacokinetics and toxicity of radiolabeled antibodies (*13–16*).

In this work we examine (a) whether the total-body tumor burden influences response or toxicity; (b) whether the patient's height, weight, or surface area influences response; (c) the relationship between the tumor absorbed dose and response; and (d) the time course of tumor volume changes. Data obtained in a series of NHL patients treated according to the Michigan protocol are used for these analyses. The first 2 items address the question of whether the mass of protein should be adjusted per patient; the last 2 investigate the dose–response relationship in patients treated by radioimmunotherapy in which significant measurable responses are seen. Data collected from the B1 antibody trials are uniquely appropriate for assessing tumor dose–response because a significant percentage of the tumors respond. This analysis represents the first comprehensive implementation of 3D-ID (*17–19*), a patient-specific, 3-dimensional (3D) dosimetry software package. As such, several dosimetric parameters that are not obtained by conventional dosimetry have been examined; these include, the minimum and maximum absorbed doses as well as a measure of dose uniformity within each tumor. The comprehensive assessment of the total-body tumor burden also reflects analysis using the 3D-ID software package, which facilitates the extraction of such information.

MATERIALS AND METHODS

Patients

Data collected from NHL patients accrued at Memorial Sloan-Kettering Cancer Center (MSKCC) that participated in 2 multicenter trials of ^{131}I-labeled anti-B1 antibody were used in the analysis: the multicenter dosimetry validation study (*4*) and the pivotal trial in chemorefractory patients (*20*). Details regarding protocol design have been published (*4,9,10,20*). Adult NHL patients with low-grade or transformed low-grade histology who had failed prior chemotherapy and who had measurable disease were eligible for the study. The therapeutic administration of labeled antibody was determined from a pretherapy tracer study to deliver a nominal whole-body absorbed dose of 75 cGy. Fifteen patients participated in these studies at MSKCC; data from 13 evaluable patients (7 men, 6 women; mean weight, 74.7 $\pm$ 17.6 kg; mean height, 169.9 $\pm$ 12.6 cm) were used in the analysis. Two patients were excluded from the analysis because they moved on to other therapies after the first follow-up visit showed rapid disease progression.

Antibody

The anti-B1 (anti-CD20) mouse immunoglobulin IgG2a antibody used in the clinical trial was provided by Coulter Pharmaceutical, Inc. (now Corixa Corp., South San Francisco, CA).

Imaging

The imaging protocol has been described previously (*11,12*). Briefly, planar, conjugate-view images acquired on the day of, and 3 and 6 d after, administration of trace-labeled ^{131}I-anti-B1 antibody were used to estimate kinetics to prescribe the therapeutic activity needed to deliver a whole-body mean absorbed dose of 75 cGy. Subsequent to therapy, planar and SPECT images were also obtained on the third or fourth day over regions identified previously to include lesions that could be seen in the tracer study and that had been identified on CT for volume determination and 3D dosimetry.

For each patient, a pretherapy (baseline) whole-body CT scan was available. CT scans were also obtained after therapy at 5- to 6-wk intervals. Scans were typically obtained with contrast and with a slice spacing of 1 cm. CT images acquired in-house were digitally transferred and converted to 3D-ID format. Film copies of images obtained at other institutions were digitized using a film digitizer (Lumiscan 75; Lumysis, Sunnyvale CA) and then provided as input to 3D-ID. MRI replaced CT in 1 patient, as warranted by the patient's site of disease.

All lesions seen on whole-body CT or on MRI were identified and volumes were obtained by drawing regions of interest (ROIs) around each lesion. Given the area of each ROI on slice i, A_i, and the slice thickness, t, the volume of each lesion, V_L, was obtained from:

$$V_L = \sum_i A_i \cdot t.$$

Whole-body tumor burden was calculated as the sum of all lesion volumes for each patient. These lesion volume estimates were also used for the conventional dosimetry performed on selected, index lesions (see below). Lesion identification and volume estimation were performed using 3D-ID.

Conventional Dosimetry

Detailed dosimetry calculations were performed for selected index lesions. These were selected on the basis of the degree to which they could be distinctly and unequivocally visualized for contour drawing on the planar imaging studies across the 3 imaging time points and also on SPECT. As many as could be so visualized were typically selected. The mean absorbed dose to index lesions was calculated as the cumulated activity concentration multiplied by the absorbed dose equilibrium constant for ^{131}I electron emissions. Because patients were treated to deliver 75 or 65 cGy to the whole body, the whole-body photon dose contribution was assumed to be the same for all lesions and was, therefore, not specifically included in the conventional dose calculations. Pharmacokinetics were obtained from the series of tracer study images. Contours were drawn on the planar nuclear medicine studies around the visible index lesions; background was estimated using contours that were adjacent to the lesions but not overlying regions of unrelated high activity concentration. The conjugate-view methodology was used to estimate tumor activity (*21*). Attenuation correction was performed using distances as measured on the CT images and an attenuation coefficient of 0.1 cm^{-1}, which was reduced from the narrow beam value of 0.11 cm^{-1} to account for scatter (*22*,*23*). The time–activity curves obtained from the planar imaging were fit to a single exponential decay function; the function was then integrated, divided by the lesion mass, and scaled by the therapeutic administration to yield the tumor cumulated activity concentration. This was multiplied by the energy emitted per decay to yield the electron absorbed dose to tumors. Estimates obtained by conventional dosimetry were used only for the comparison with 3D-ID–derived estimates. All dose–response analyses were performed with 3D-ID–derived tumor dose estimates.

Patient-Specific, SPECT-Based Dosimetry

Patient-specific dosimetry was performed using a previously described software package, 3D-ID (*18*). The following steps are required in such dose calculations: (a) SPECT and CT images are registered to ensure a match between the lesion as seen on SPECT and the lesion as identified on CT. (b) ROIs are drawn on each CT slice to define lesion volumes. (c) Cumulated activities, obtained from planar imaging, as described above, are assigned to each lesion volume. (d) A point-dose kernel for ^{131}I photons is convolved with the spatial distribution of activity as obtained from SPECT; electrons are assumed to be locally deposited. SPECT and CT image registration was performed using the Pelizzari–Chen software package (*24*) and a software package, MIAU, which was recently developed in-house (*25*,*26*). The spatial distribution of absorbed dose was used to obtain the mean absorbed dose and also dose–volume histograms over the lesion volume. It is important to note that because multiple SPECT images were not typically acquired, planar imaging was used to obtain the pharmacokinetics required for estimating cumulated activity. By scaling the total counts in each SPECT tumor ROI to the cumulated activity of each tumor, the implicit assumption is made that the spatial distribution measured at the time at which SPECT was undertaken was constant but that the kinetics followed those measured by planar imaging. For example, if the activity concentration ratio in portion A of the tumor is measured to be 2-fold greater than that in portion B of the tumor, that relationship is assumed constant throughout the uptake and clearance kinetics so that the same cumulated activity ratio would then also apply.

Toxicity Assessments

Hematologic toxicity was assessed using the National Cancer Institute common toxicity criteria. Toxicity grades were obtained for platelets, neutrophils, and leukocytes. The impact of height, weight, surface area, and plasma volume on toxicity was examined.

Plasma volume (V) was estimated from each patient's height and weight using the following equations (*27*): For males, $V = 23.7\,H + 9.0\,W - 1709$; and for females, $V = 40.5\,H + 8.4\,W - 4811$, with V in millimeters when the height, H, and the weight, W, are in centimeters and kilograms, respectively.

Statistical Analysis

The Spearman rank correlation coefficient was used to assess any strong monotonic associations between dosimetry parameters (e.g., mean, maximum, minimum and uniform absorbed dose) and volume parameters (e.g., volume reduction at days 35, 75, 120, and initial volume). This measure is calculated on the basis of the ranks and is more appropriate when the data consist of extreme values or outliers. A nonparametric test was computed to determine whether the correlation coefficient was statistically significant at the 5% level (*28*). The software package SAS (Carey, NC) was used for all statistical analyses.

RESULTS

Figure 1 depicts whole-body and planar spot images of ^{131}I-anti-B1 antibody distribution after therapeutic administration.

The time course of total tumor burden for each patient is presented in Figure 2. A large variation in the total tumor burden response may be seen. Over the relatively short time period examined, the total tumor burden in patients 1, 3, 8–10, and 13 was reduced. In patients 5–7, 12, and 14, the initial drop was followed by an increase. In some patients, patients 5, 6, and 14, the increase was rapid, appearing within or shortly after 10 wk after therapy. In patients 4 and 15, no decrease in tumor burden was observed as a result of therapy.

Dosimetry Analysis

Results from the dosimetry analysis are presented in Table 1 and Figure 3. To illustrate the type of data collected, Table 1 lists results obtained for 7 patients and 16 distinct index tumors. Lesion volume estimates, before treatment and at 35 and 75 d, after treatment, are shown along with absorbed dose estimates calculated by conventional means and by 3D-ID. For all patients, the tumor dose calculated using 3D-ID ranged from 0.37 to 17.6 Gy, with a median of 3 Gy. Figure 3 depicts histograms representing the spatial distribution of absorbed dose for 6 different tumors in a single patient. The results are scaled to the maximum dose calculated for each tumor volume. The variability in dose distribution within several tumors of a single patient is shown. Sharply dropping curves indicate a more uniform distribution of absorbed dose, whereas curves with a lower slope correspond to a decreased spatial uniformity in absorbed dose.

Figures 4–6 examine possible relationships between absorbed dose, initial tumor volume, and response. In Figure

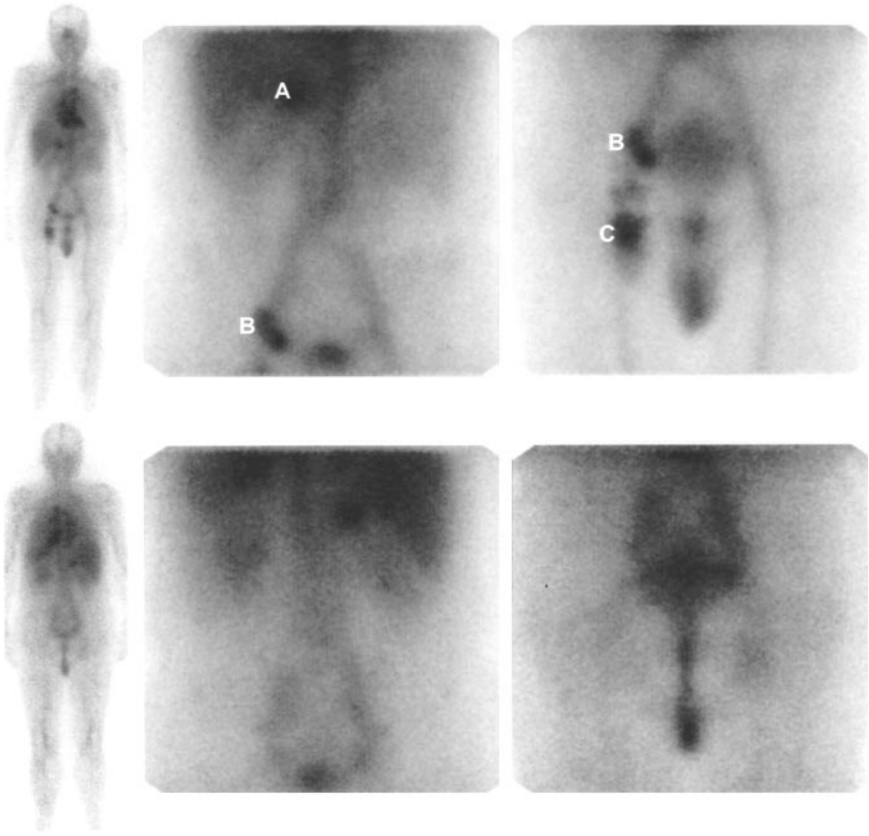

FIGURE 1. Images of ^{131}I-anti-B1 antibody distribution 3 d after therapeutic administration of 2.7 GBq. Anterior and posterior views are shown in first and second rows of images, respectively. First column shows whole-body views; second and third columns depict abdominal and pelvic views, respectively. Right adrenal (A), inguinal (B), and femoral (C) masses may be seen in images. Abdominal and pelvic views overlap so that inguinal mass (B) is seen in both images. In pelvic view, bladder may be seen adjacent to inguinal mass. Each image is scaled to maximum pixel intensity in view; bladder does not appear on abdominal view because of high activity level in upper abdomen.

4, the percentage reduction in tumor volume is plotted against the mean (Fig. 4A), maximum (Fig. 4B), and minimum (Fig. 4C) absorbed dose; a measure of the uniformity in the spatial distribution of absorbed dose is also examined and has been parameterized as the ratio of the minimum to maximum absorbed doses (Fig. 4D). The percentage reduction in tumor volume at 35, 75, and 120 d after treatment is plotted against each of the dosimetric parameters listed above. A trend toward increased response with increasing uniformity was observed ($r = 0.37$; $P = 0.06$); otherwise, no statistically significant correlation was observed between tumor volume reduction and any of the parameters examined for any of the days considered after therapy ($P = 0.25$ to $P > 0.5$).

The relationship between absorbed dose or percentage uptake per gram and lesion volume has been examined by several investigators (*29–31*). As shown in Figure 5A, a trend toward increased absorbed dose with decreasing tu-

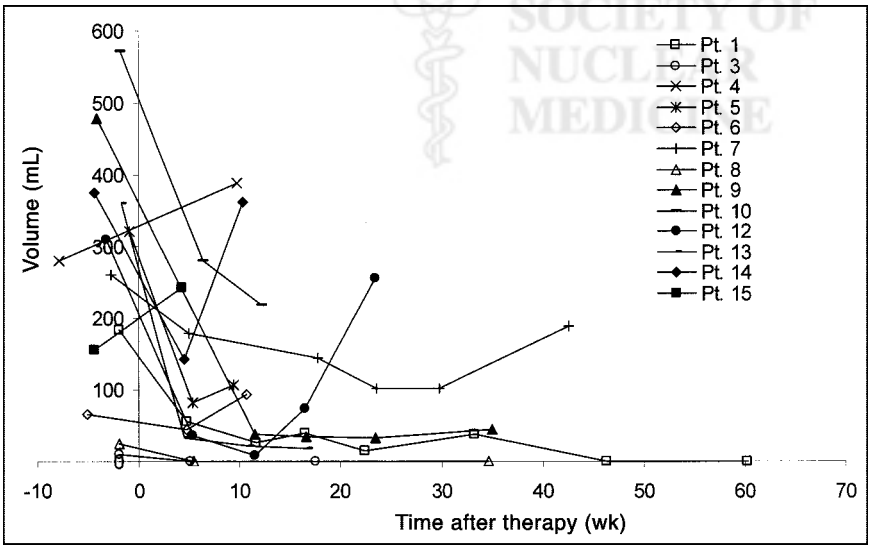

FIGURE 2. Total tumor burden vs. follow-up time, after treatment, is plotted. Treatment time is at $t = 0$; therefore, pretreatment burden estimates are shown at $t < 0$. Pt. = patient.

TABLE 1
Sample of Data Collected for Abridged, But Representative, List of Index Lesions

Tumor name	Tumor volume (mL)			Mean dose (Gy)	
		Post-TX			
	Pre-TX	Day 35	Day 75	Conv.	3D-ID
L common iliac	26.4	18.8	0	2.2	2.3
L external iliac	46.3	16.7	13.7	12.9	13.5
R external iliac	30.3	0	4	1.5	2.2
L external iliac	22.6	3.6	0	2.37	2.2
R inguinal	18.3	4.8	6.5	1.8	1.96
L inguinal	29.9	2.2	3.1	0.34	0.37
R adrenal	14.5	14.4	7.2	12.1	12.8
R femoral	27.1	0	48.7	9.1	10.2
R inguinal 1	9.2	5.7	24.1	15.7	16.4
R inguinal 2	7.2	0	0	13	13.5
L axillary	38.3	4.5	0	0.7	0.7
R obturator	9.5	0	0	3.8	3.9
R external iliac	13.1	0	0	3.9	4.1
Mesenteric	75.3	0	0	2	2.2
L paraaortic	135	26.2	28.9	1.3	1.4
Retrocaval	41.6	18.9	15.19	2.8	3
L paraaortic	55	7	14.98	6.8	7.2

Pre-TX = before treatment; Post-TX = after treatment; Conv. = conventional.

mor volume is observed in these studies ($r = -0.27$; $P = 0.14$). However, this did not achieve statistical significance and, as shown in Figure 5B ($P > 0.5$), it did not translate into a better response for small versus large lesions.

Because the total protein mass of antibody administered to all patients in the studies was constant, patients with larger tumor burdens might be expected to have reduced responses because the greater tumor burden would bind a greater fraction of the administered antibody and, therefore, yield a reduced concentration of circulating radiolabeled antibody relative to that in patients with minimal burdens (*16*). This possibility was examined by plotting the percentage reduction in total tumor volume against the initial total-body tumor burden (Fig. 6). The best response, corresponding to the nadir of the total tumor burden, as well as the response assessment after 120 d, was examined. No relationship was seen between the initial total-body burden and tumor burden reduction ($P = 0.34$).

Toxicity Correlations

In patients with minimal disease and, therefore, a greater circulating concentration of antibody, increased hematologic toxicity might be predicted because of an excess of circulating radiolabeled antibody. This was examined by plotting toxicity against tumor burden (Fig. 7A). No correlation was observed. The possibility that the patient's

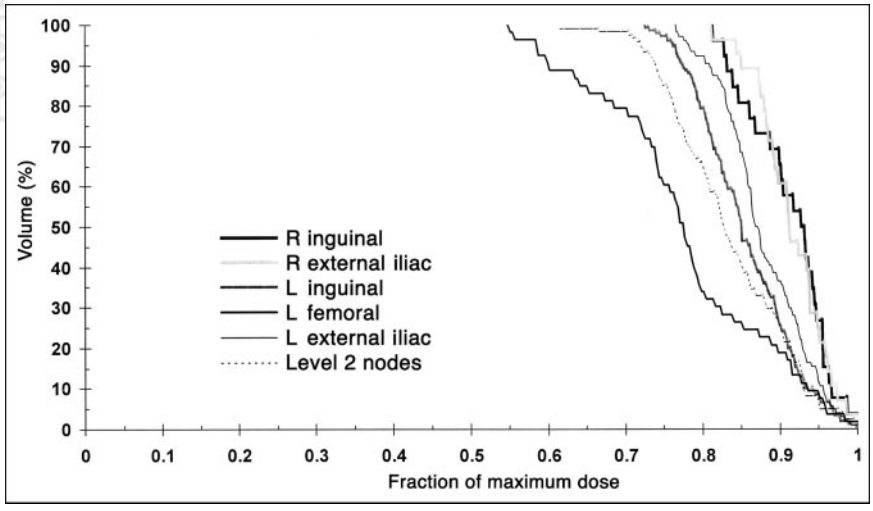

FIGURE 3. Dose–volume histograms represent spatial distribution of absorbed dose for 6 different index lesions in 1 patient. Percentage of lesion volume receiving absorbed dose that is greater than or equal to *x*-axis value obtained from each curve is shown. Histograms have been scaled so that maximum dose for each lesion is equal to 1.

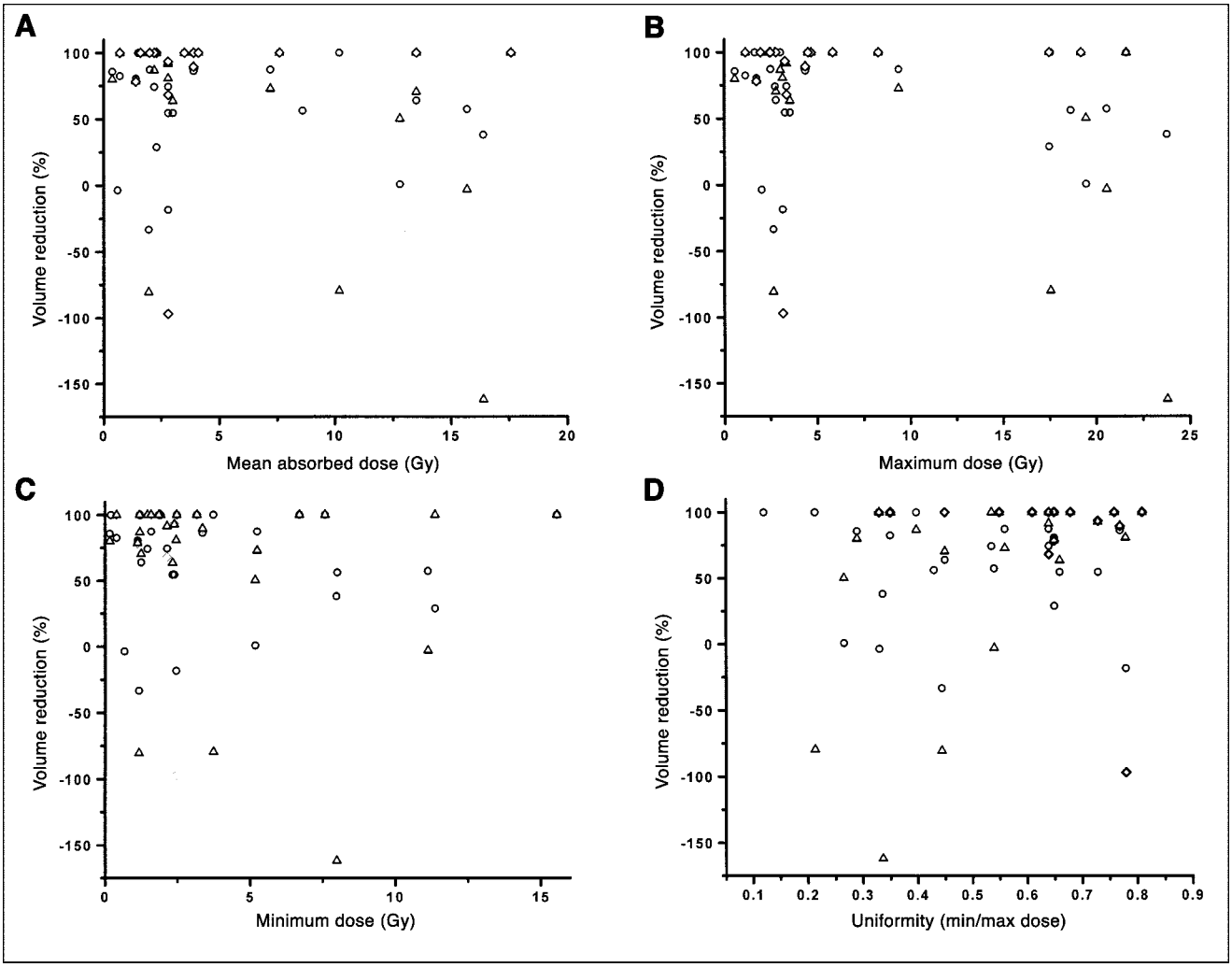

FIGURE 4. Percentage reduction in index lesion volumes at 35 (○), 75 (△), and 120 (◇) d after treatment is plotted against mean (A), maximum (B), and minimum (C) absorbed dose and against measure of spatial uniformity in absorbed dose (min/max absorbed dose within each index lesion) (D).

height, weight, surface area, or calculated plasma volume might influence response or toxicity given a constant administered milligram amount of antibody was also examined (Figs. 7B–7E). No correlation was seen for any of these parameters ($P > 0.5$).

DISCUSSION

Radioimmunotherapy of NHL with ^{131}I-anti-B1 has produced durable complete responses in patients with relapsed and refractory disease. A detailed dosimetric analysis has been performed to examine whether 1 of the 2 currently implemented standard protocols for the anti-B1 antibody would yield superior results if modified to better account for individual patient characteristics, such as tumor burden or height and weight. Using a dosimetry package, 3D-ID, which provides the spatial distribution of the absorbed dose in addition to the mean absorbed dose for tumor volumes, dose–response relationships were also examined for selected, index lesions.

The time course of the total tumor burden changes after radioimmunotherapy has not been examined previously in patients. As seen in Figure 3, no prognostically relevant pattern was observed to suggest, for example, that a rapid initial drop in tumor burden yielded more favorable responses.

In a similar, but previously untreated, patient population and using the same antibody and treatment approach, Koral et al. (*32*) examined tumor absorbed dose versus response by comparing the tumor absorbed dose for tumors in patients with partial versus those with complete responses. Such measures of response reflect the overall clinical condition of the patient because they are influenced by whether or not new lesions have appeared. Using a mixed ANOVA technique, a trend toward a significant difference was observed. In a more recent report, Koral et al. (*33*) examined volume reduction in a restricted dataset: patients with abdominal or pelvic SPECT scans who had achieved a partial response. Volume reduction changes were examined after

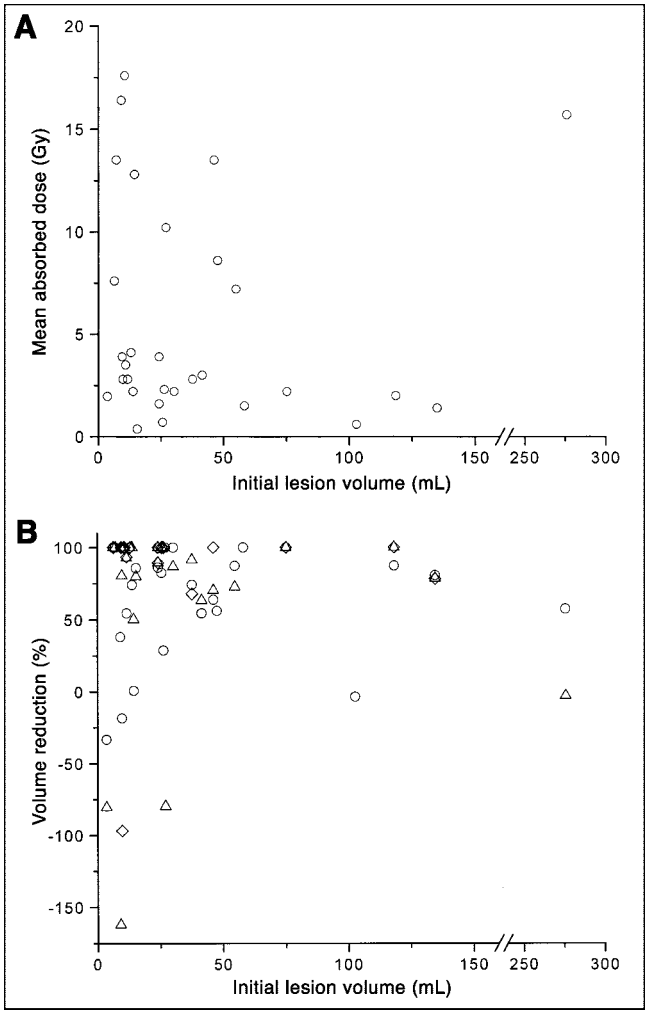

FIGURE 5. (A) Mean absorbed dose delivered to each index lesion is plotted against initial index lesion volume. (B) Percentage reduction in index lesion volume at 35 (○), 75 (△), and 120 (◇) d after treatment is plotted against initial volume of each index lesion.

12 wk. Two different methods were used for defining tumor volumes and 2 different methods were used for estimating absorbed dose. Depending on the subgroup of patients examined, and the methods used, different dose–response relationships were found. In no case was a statistically significant relationship observed. In our study, all evaluable patients were included in the analysis and similar observations were found. That no relationship was observed may be explained, in part, by the effects of prior treatment, which would be expected to differentially impact tumor radiosensitivity and, thereby, confound an absorbed dose–response relationship (*34*). Another possible explanation is the potential therapeutic efficacy of the naked antibody (*35*). This component of potential therapeutic effect is not accounted for in the absorbed dose estimate. It is also important to note that dose-rate effects were not considered in this analysis. Dose–response results obtained in patients with malignant glioma, treated with ^{131}I-labeled 81C6 (antitenascin) antibody, have shown that the dose rate can influence the therapeutic outcome in radioimmunotherapy in a manner similar to that seen with external radiotherapy and brachytherapy (*36*). A possible dose-rate effect has also been observed for marrow toxicity in the murine model (*37*). Finally, the poor dose and toxicity correlations may indicate that the absorbed dose delivered is too low to yield any significant dose–response relationship. In the dose range 0–600 Gy, dose–response relationships have been observed for ^{90}Y-labeled peptides (*38*).

In the relatively small patient population examined, tumor burden and height or weight of the patient did not influence the response of index lesions or hematologic toxicity. As discussed earlier, tumor burden might have impacted the availability of circulating antibody and, thereby, antibody localization to tumors or hematologic toxicity. The patient's height and weight may be used to estimate the patient's surface area or plasma volume. These parameters might also impact on the concentration of radiolabeled antibody in the circulation. Because response was not influenced by these parameters, patient-specific dosing of unlabeled antibody is not likely to yield improved responses. It is possible that the influence that tumor burden would have on the protein mass of antibody needed to improve response is masked by the existence of a large pool of nonspecific binding sites in the reticuloendothelial system. Antigen sites associated with total-body tumor may be a small fraction of the total sites to which administered antibody will bind. If this were the case, then beyond a certain level of administered antibody, the sensitivity to changes in tumor burden would be too low to uncover in a relatively small patient study.

CONCLUSION

This analysis represents the first full implementation of the patient-specific 3D dosimetry package, 3D-ID. The ab-

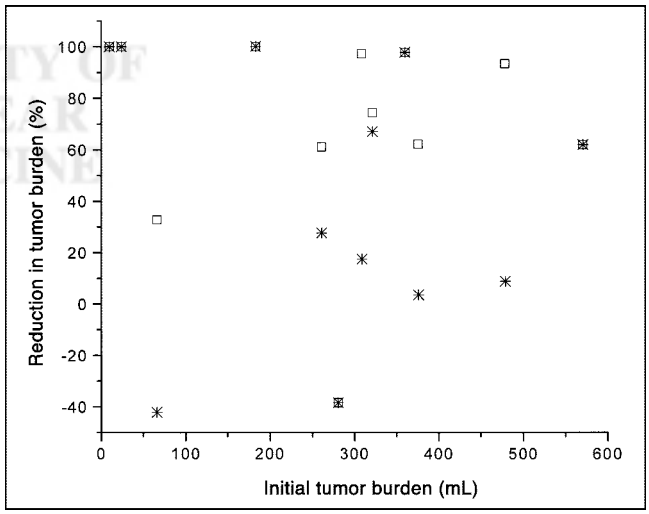

FIGURE 6. Percentage reduction in overall tumor burden at nadir of tumor burden (□) and after 120 d (✳) is plotted against initial total-body tumor burden of each patient.

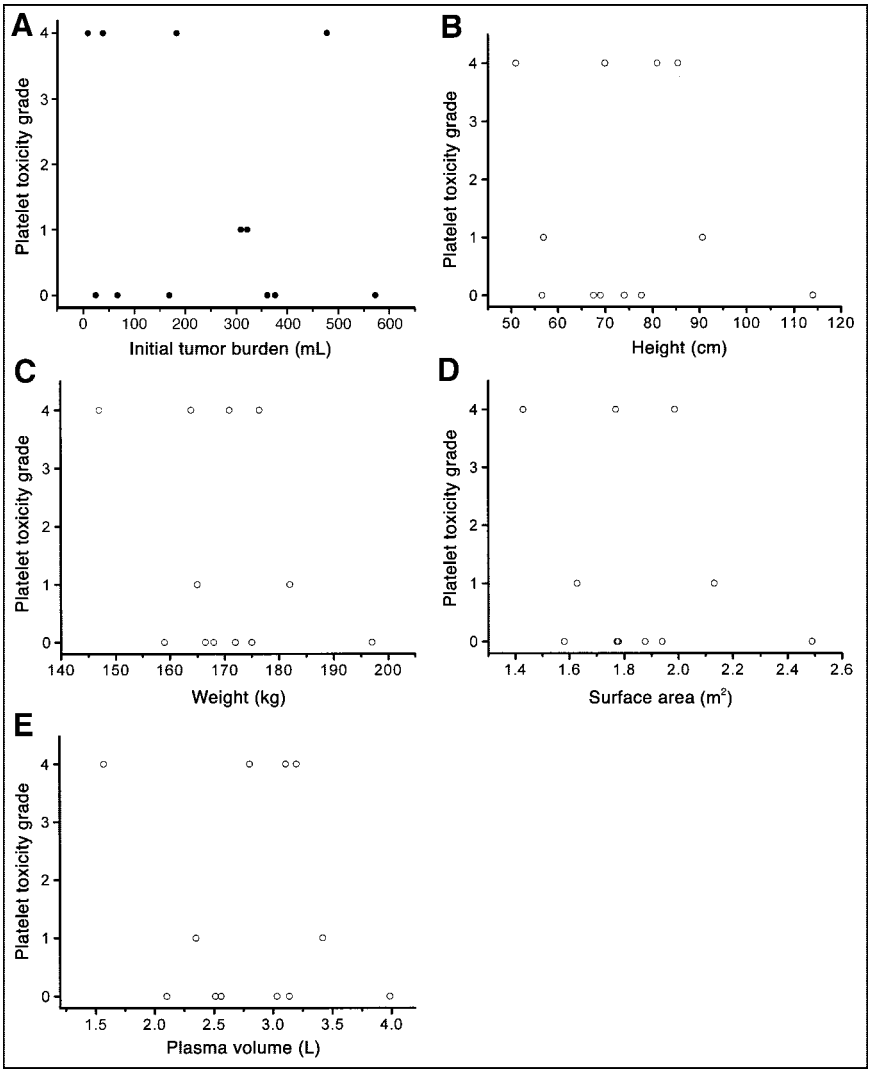

FIGURE 7. Platelet toxicity grade is plotted against initial total-body tumor burden (A), height (B), weight (C), body surface area (D), and calculated plasma volume (E).

sence of a dose–response relationship for tumors is surprising and suggests that absorbed dose is not the sole determinant of tumor response in these patients. The absence of a correlation between the total-body tumor burden and the overall response or toxicity suggests that tailoring the milligram amount of administered antibody to patient tumor burden is not likely to improve response or reduce toxicity.

ACKNOWLEDGMENTS

The assistance of Peter Karp, the Research Study Assistant on the protocol, is acknowledged. This work was supported, in part, by National Institutes of Health grant R01 CA62444, by Department of Energy grant DE-FG02–86ER60407, and by Coulter Pharmaceutical, Inc. (now Corixa Corp.).

REFERENCES

1. Kaminski MS, Zasadny KR, Francis IR, et al. Radioimmunotherapy of B-cell lymphoma with [^{131}I]anti-B1 (anti-CD20) antibody. *N Engl J Med.* 1993;329:459–465.
2. Press OW, Eary JF, Appelbaum FR, et al. Radiolabeled-antibody therapy of B-cell lymphoma with autologous bone marrow support. *N Engl J Med.* 1993;329:1219–1224.
3. Moskowitz CH. Conventional treatments for non-Hodgkin's lymphoma: the need for new therapies. *J Nucl Med.* 1998;39(8 suppl):2S–10S.
4. Vose JM, Wahl RL, Saleh M, et al. Multicenter phase II study of iodine-131 tositumomab for chemotherapy-relapsed/refractory low-grade and transformed low-grade B-cell non-Hodgkin's lymphomas. *J Clin Oncol.* 2000;18:1316–1323.
5. Kaminski MS, Estes J, Zasadny KR, et al. Radioimmunotherapy with iodine ^{131}I tositumomab for relapsed or refractory B-cell non-Hodgkin lymphoma: updated results and long-term follow-up of the University of Michigan experience. *Blood.* 2000;96:1259–1266.
6. Wiseman GA, White CA, Witzig TE, et al. Radioimmunotherapy of relapsed non-Hodgkin's lymphoma with Zevalin, a ^{90}Y-labeled anti-CD20 monoclonal antibody. *Clin Cancer Res.* 1999;5(10 suppl):3281s–3286s.
7. Witzig TE, White CA, Wiseman GA, et al. Phase I/II trial of IDEC-Y2B8 radioimmunotherapy for treatment of relapsed or refractory CD20(+) B-cell non-Hodgkin's lymphoma. *J Clin Oncol.* 1999;17:3793–3803.
8. Kaminski MS, Estes J, Tuck M, et al. Iodine-131-tositumomab therapy for previously untreated follicular lymphoma. Proceedings of the American Society of Clinical Oncology; May 20–23, 2000; New Orleans, LA. Abstract 11:5a.
9. Eary JF, Press OW, Badger CC, et al. Imaging and treatment of B-cell lymphoma. *J Nucl Med.* 1990;31:1257–1268.
10. Kaminski MS, Zasadny KR, Francis IR, et al. Iodine-131-anti-B1 radioimmunotherapy for B-cell lymphoma. *J Clin Oncol.* 1996;14:1974–1981.
11. Wahl RL, Kroll S, Zasadny KR. Patient-specific whole-body dosimetry: principles and a simplified method for clinical implementation. *J Nucl Med.* 1998;39(8 suppl):14S–20S.

12. Wahl RL. Iodine-131 anti-B1 antibody therapy in non-Hodgkin's lymphoma: dosimetry and clinical implications. *J Nucl Med.* 1998;39(8 suppl):1S.
13. Blumenthal RD, Fand I, Sharkey RM, Boerman OC, Kashi R, Goldenberg DM. The effect of antibody protein dose on the uniformity of tumor distribution of radioantibodies: an autoradiographic study. *Cancer Immunol Immunother.* 1991; 33:351–358.
14. Boerman OC, Sharkey RM, Wong GY, Blumenthal RD, Aninipot RL, Goldenberg DM. Influence of antibody protein dose on therapeutic efficacy of radioiodinated antibodies in nude mice bearing GW-39 human tumor. *Cancer Immunol Immunother.* 1992;35:127–134.
15. Boerman OC, Sharkey RM, Blumenthal RD, Aninipot RL, Goldenberg DM. The presence of a concomitant bulky tumor can decrease the uptake and therapeutic efficacy of radiolabeled antibodies in small tumors. *Int J Cancer.* 1992;51:470–475.
16. Yu B, Carrasquillo J, Milenic D, et al. Phase I trial of iodine 131-labeled COL-1 in patients with gastrointestinal malignancies: influence of serum carcinoembryonic antigen and tumor bulk on pharmacokinetics. *J Clin Oncol.* 1996;14:1798–1809.
17. Sgouros G, Chiu S, Pentlow KS, et al. Three-dimensional dosimetry for radioimmunotherapy treatment planning. *J Nucl Med.* 1993;34:1595–1601.
18. Kolbert KS, Sgouros G, Scott AM, et al. Implementation and evaluation of patient-specific three-dimensional internal dosimetry. *J Nucl Med.* 1997;38:301–308.
19. Furhang EE, Chui CS, Kolbert KS, Larson SM, Sgouros G. Implementation of a Monte Carlo dosimetry method for patient-specific internal emitter therapy. *Med Phys.* 1997;24:1163–1172.
20. Kaminski MS, Zelenetz AD, Press OW, et al. Pivotal study of iodine I 131 tositumomab for chemotherapy-refractory low-grade or transformed low-grade B-cell non-Hodgkin's lymphomas. *J Clin Oncol.* 2001;19:3918–3928.
21. Thomas SR, Maxon HR, Kereiakes JG. In vivo quantitation of lesion radioactivity using external counting methods. *Med Phys.* 1976;3:253–255.
22. Hubbell JH, Seltzer SM. X-ray Mass Attenuation Coefficients: National Institutes of Standards and Technology Web site. 1996. Available at: http://www.physics.nist.gov/PhysRefData/Xcom/Text/XCOM.html. Accessed September 27, 2001.
23. Grant EJ. *A Triple Energy Window Method for In-Vivo Quantitation of Iodine-131 from Anger Camera Images* [master's thesis]. Houston, TX: University of Texas; 1994:40–43.
24. Pelizzari CA, Chen GT, Spelbring DR, Weichselbaum RR, Chen CT. Accurate three-dimensional registration of CT, PET, and/or MR images of the brain. *J Comput Assist Tomogr.* 1989;13:20–26.
25. Kolbert KS, Sgouros G. Display and manipulation of SPECT and CT studies for radiolabeled antibody therapy [abstract]. *Cancer Biother Radiopharm.* 1998;13: 302.
26. Kolbert KS, Hamacher KA, Jurcic JG, Scheinberg DA, Larson SM, Sgouros G. Parametric images of antibody pharmacokinetics in Bi213-HuM195 therapy of leukemia. *J Nucl Med.* 2001;42:27–32.
27. Snyder WS, Cook MJ, Nasset ES, Karhausen LR, Howells GP, Tipton IH. *Report of the Task Group on Reference Man.* ICRP publication 23. Elmsford, NY: International Commission on Radiological Protection; 1975.
28. Glantz SA. *Primer of Biostatistics*. 2nd ed. New York, NY: McGraw Hill; 1987:230–234.
29. Yoshida K, Rivoire ML, Divgi CR, Niedzwiechi D, Cohen AM, Sigurdson ER. Effect of tumor size on monoclonal antibody uptake in a metastatic model. *J Surg Oncol.* 1992;49:249–252.
30. Williams LE, Bares RB, Fass J, Hauptmann S, Schumpelick V, Buell U. Uptake of radiolabeled anti-CEA antibodies in human colorectal primary tumors as a function of tumor mass. *Eur J Nucl Med.* 1993;20:345–347.
31. Behr TM, Sharkey RM, Juweid ME, et al. Variables influencing tumor dosimetry in radioimmunotherapy of CEA-expressing cancers with anti-CEA and antimucin monoclonal antibodies. *J Nucl Med.* 1997;38:409–418.
32. Koral KF, Dewaraja Y, Clarke LA, et al. Tumor-absorbed-dose estimates versus response in tositumomab therapy of previously untreated patients with follicular non-Hodgkin's lymphoma: preliminary report. *Cancer Biother Radiopharm.* 2000;15:347–355.
33. Koral KF, Francis IR, Kroll S, Zasadny KR, Kaminski MS, Wahl RL. Volume reduction versus radiation dose for tumors in previously untreated lymphoma patients who received iodine-131 tositumomab therapy: conjugate views compared with a hybrid method. *Cancer.* 2002;94(4 suppl):1258–1263.
34. Williams LE. Clinical results and the necessity of estimating patient-specific radiation absorbed dose in radioimmunotherapy [comment on letter]. *Cancer Biother Radiopharm.* 2000;15:301–303.
35. Cardarelli P, Quinn M, Colcher D, Bebbington C, Yarranton G. Induction of apoptosis and inhibition of cellular proliferation of human B-cell lines by anti-CD20 antibodies, tositumomab and rituximab. Proceedings of the American Society of Clinical Oncology; May 12–15, 2001; San Fransisco, CA. Abstract 1096.
36. Akabani G, Cokgor I, Coleman RE, et al. Dosimetry and dose-response relationships in newly diagnosed patients with malignant gliomas treated with iodine-131-labeled anti-tenascin monoclonal antibody 81C6 therapy. *Int J Radiat Oncol Biol Phys.* 2000;46:947–958.
37. Behr TM, Memtsoudis S, Sharkey RM, et al. Experimental studies on the role of antibody fragments in cancer radio-immunotherapy: influence of radiation dose and dose rate on toxicity and anti-tumor efficacy. *Int J Cancer.* 1998;77:787–795.
38. Jonrad P, Jamar F, Walrand S, et al. Tumor dosimetry based on PET ^{86}Y-DOTA-TYR^{3}-octreotide (SMT487) and CT-scan predicts tumor response to ^{90}Y-SMT487 (Octreother^{tm})[abstract]. *J Nucl Med.* 2000;41(suppl):111P.